To Appear MEMS94

A COMPUTATIONALLY PRACTICAL APPROACH TO SIMULATING COMPLEX SURFACE-MICROMACHINED STRUCTURES WITH FABRICATION NON-IDEALITIES

H. Yie[†], S. F. Bart[‡], J. White, and S. D. Senturia
Department of Electrical Engineering and Computer Science,
Massachusetts Institute of Technology, Cambridge, MA.
[†]Now with Intellisense, Inc., Wilmington, MA.
[‡]Analog Devices, Inc., Wilmington, MA.

Abstract

The objective of this work was to develop methods which would allow the electromechanical analysis of a Microelectromechanical System (MEMS) structure with the level of complexity of a practical, high-volume manufacturable sensor while avoiding computationally impractical models. Two methods were developed. One was a simple analysis method in which the ideal structure was assumed. This allowed prediction of the stability and the effects of structure misalignment on a surface-micromachined accelerometer. However, the simple method is limited because the actual structure has fabrication induced non-idealities, such as warpage, which can cause the simple method to be significantly in error. The second method discarded the ideal structure assumption and analyzed the non-ideal structure via a self-consistent analysis. This method is based on the calculation of an intermediate look-up table from which the electrostatic forces are obtained directly from the position of the moving mass, greatly reducing computation time and memory requirements in comparison to a standard self-consistent electromechanical analysis scheme. Using this lumped-model self-consistent scheme, we analyzed an Analog Devices, Inc. ADXL50 accelerometer including fabrication non-idealities (warpage, overetching, residual stress, etc.). For this structure the lumped-model self-consistent analysis method reduced the required number of electrostatic analysis discretization panels by a factor of about 100. Computation times were typically 5–7 hours instead of a predicted time of more than a month for a standard self-consistent electromechanical analysis scheme. Further, memory requirements for the standard method would have significantly exceeded practical limitations. The electromechanical resonant frequency was measured for several ADXL50 accelerometers and compared to the simulation results showing good agreement.

1 Introduction

Surface micromachined accelerometers are increasingly being used as high reliability, low cost replacements for present electromechanical accelerometers. To improve linearity, these accelerometers are often closed-loop, force-rebalance devices in which applied voltages create electrostatic forces to balance the mechanical forces and the inertial force due to acceleration. Fig. 1 is a schematic diagram of the electromechanical sensor portion of the prototype, low-g, surface micromachined accelerometer examined here. The structure of the sensor consists of 50 fixed and moving finger "unit cells". The fixed fingers are attached to the substrate and do not move. The moving fingers are attached to the moving mass which is suspended by four folded tethers. Also examined in this work is the Analog Devices, Inc. ADXL50 accelerometer structure, which is similar except that its tethers are straight (see Fig. 3) [1].

Each finger cell forms a pair of series capacitors. An acceleration causes the moving mass and its fingers to move, creating imbalances in the series capacitor pairs. During normal operation each set of fixed fingers has a DC bias voltage of 3.4 and 0.2 volts respectively and the moving mass has a DC bias voltage of 1.8 volts. In addition, 0.6 volt (peak-to-peak), 1 MHz, antiphase square waves are superimposed on the DC bias of the fixed fingers. This 1 MHz signal is capacitively coupled to the moving beam in proportion to its distance from its neutral position. This signal is then demodulated and amplified to yield the output signal. The output signal is also used as a feedback signal which alters the moving beam voltage and thus applies an electrostatic force which keeps the moving beam centered [2].

The structures in Fig. 1 and Fig. 3 imply 3-D extrusions of ideal 2-D layouts. However, when these structures are fabricated, many non-idealities occur. In the case of the ADXL50, the most prominent non-ideality is warpage in the structural poly-silicon layer which is due to a residual stress gradient across the thickness of the

film. In addition, there are effects due to over-etching, mask misalignment, and average residual stress.

To predict and analyze these devices' performance, we require electromechanical analysis. However, because of the large aspect ratios and fundamentally 3-D nature of complex surface micromachined structures, their analysis often requires an excessive number of nodes or panels in a standard electro-mechanical self-consistent analysis scheme [3]. To overcome this problem, we have developed two analysis methods. Both methods use the finite-element mechanical solver ABAQUS [4] and the fast multipole-accelerated boundary-element electrostatic solver FastCap [5]. The simple analysis method assumes that the fabrication induced warpage can be ignored and thus all the unit cells in the sensor portion are identical. However, the fabrication induced warpage can make the cells significantly different from each other in which case the simple analysis method can yield unsatisfactory analysis results. The lumped-model self-consistent scheme overcomes this difficulty and deals with each unit cell individually. Using the lumped-model self-consistent method, we analyzed the electromechanical resonant frequency of the ADXL50 accelerometer, and compared the results to experimentally measured data.

2 Simple Analysis Method

The simple analysis scheme assumes an ideal, flat structure. Each of the unit cells are identical, so one cell can be analyzed and the results multiplied by the total number of cells to get the structural response. In spite of this limitation, several useful results can be obtained. The computations are performed as follows. First, extract the dependence of the 3-D capacitance matrix on the displacement for a unit cell and evaluate the electrostatic force F_E versus the displacement for the total structure using the relation:

$$F_E = \frac{N}{2}\frac{\partial}{\partial x}\sum_{i,j} C_{i,j} {V_{i,j}}^2 \tag{1}$$

where N is the cell number, $C_{i,j}$ is a capacitance matrix element, and $V_{i,j}$ is the potential difference between conductor i and j. Second, by defining F_M as the mechanical force, M as the moving beam mass, and a as the applied acceleration, from

$$F_M(x) + F_E(x, V) = Ma \tag{2}$$

given the applied voltage, we can calculate the displacement, x, versus the acceleration, a. Also, setting the displacement, x, we can obtain the relationship between the applied feedback voltage and the acceleration.

This simple method allowed a comparison of the slope of the tether force versus displacement to the slope of the electrostatic force versus displacement. This is a critical comparison since the slope of the tether force must be larger than that of the electrostatic force to assure stability.

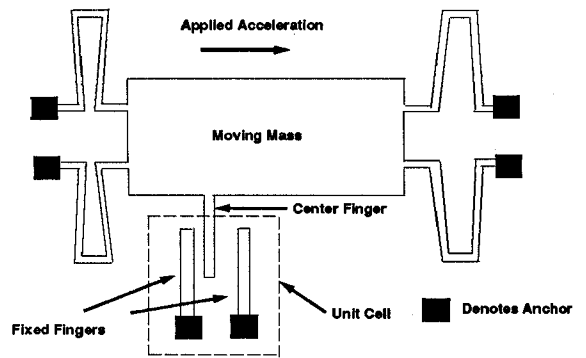

Figure 1: Schematic diagram of the low-g accelerometer sensor displaced by an applied acceleration

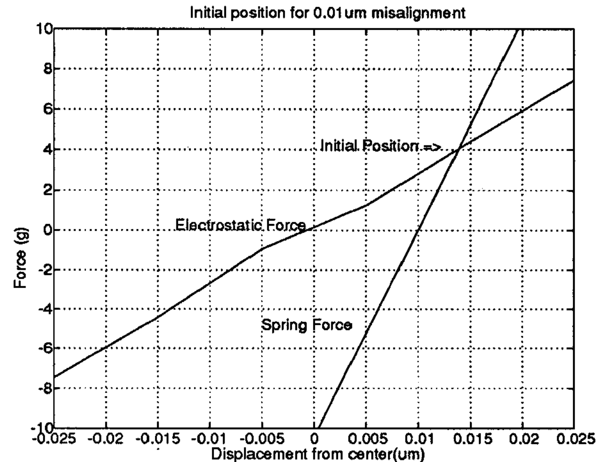

Figure 2: Forces versus displacement for 0.01 μm mask misalignment.

The simple analysis method also allowed examination of the effect of small structural misalignments due to fabrication, etc. Fig. 2 plots the curves of electrostatic force and tether spring force versus the displacement from the center position for the low-g structure (Fig. 1) with a 0.01 μm moving mass misalignment along the acceleration axis. From the intersection of the two curves (the equilibrium position), we find that a 0.01 μm misalignment will induce a voltage offset equivalent to a 4g acceleration offset. Thus, due to the electrostatic forces caused by the DC bias voltages, the actual equilibrium position is 40% further from the center than the misalignment would indicate. Such analyses are extremely important for reducing costly prototype failures due to electromechanically enhanced non-idealities such as structure misalignment.

3 Lumped-model Self-consistent Analysis Method

The simple analysis method assumes that all the unit cells in the sensor structure are identical. However, due to the fabrication induced warpage, each unit cell has a

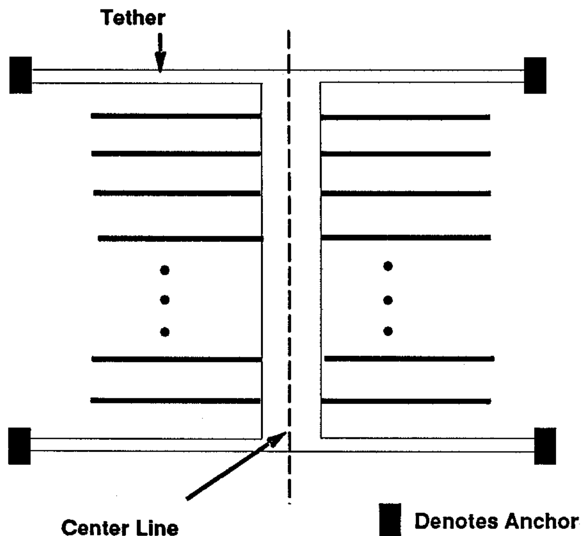

Figure 3: Schematic diagram of the ADXL50 moving mass.

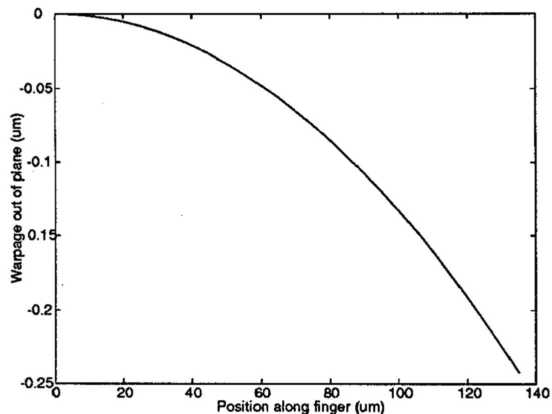

Figure 4: Simulated warpage of a fixed finger cantilever.

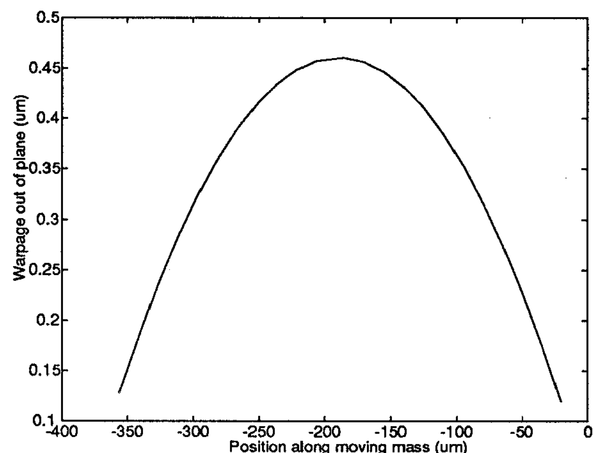

Figure 5: Simulated warpage of the moving mass along the cross section.

different force contribution to the displacement of the total moving structure. Since the fingers are stiff relative to the tether, we can apply the cell electrostatic force vector at the intersection center of the moving finger and the moving mass. On the basis of this idea, we developed the lumped-model self-consistent analysis method as follows. First, we model the fabrication induced residual stress gradient and its associated warpage. This allows us to obtain the system's static shape. The residual stress gradient which causes the warpage was modeled as a thermal gradient of 26.5 deg. with a thermal expansion coefficient of $2.0 \times 10^{-6}(deg.^{-1})$. These thermal parameters were obtained by matching the maximum simulated tip deflection of a fixed finger and the maximum simulated height of the center of the moving mass to average measured values for many hundreds of ADXL50 structures. Fig. 4 plots the simulated warpage of a typical cantilever finger of length 135 μm. Fig. 5 plots the simulated warpage along the center line of the ADXL50 accelerometer's moving mass (see Fig. 3). Note that other fabrication induced effects such as over-etching and misalignment are taken into account in the definition of the initial model geometry.

The second step requires calculating the cell electrostatic energy by using FastCap to compute the capacitance matrix in the relation

$$E = \frac{1}{2}\sum_{i,j} C_{i,j} V_{i,j}^{2}. \tag{3}$$

Fig. 6 shows the FastCap mesh for a finger cell. Since these accelerometer structures are designed to be much stiffer in the non-sensitive in-plane axis (y axis), we assume that the moving mass can move in the acceleration sensitive axis (x axis) and the out-of-plane, or levitation axis (z axis). The electrostatic energy is thus differentiated with respect to the x and z displacements to build a table of cell electrostatic force versus finger position values. Fig. 7 shows the electrostatic energy distribution which was differentiated to build the force versus position table. Next, for each finger's position, the x and z axis electrostatic force components from the lumped-model table are attached to the moving mass structural model. Finally, we self-consistently analyze the structural model with the applied finger forces using ABAQUS. The final two steps are repeated until the displacement stops changing.

Using strict mathematical theory [6], we have shown that the lumped-model self-consistent analysis scheme will converge if

$$\left|\frac{\partial F_M}{\partial F_E}\frac{\partial F_E}{\partial d}\right| < 1 \tag{4}$$

where d is the moving finger displacement. Physically, $\frac{\partial F_E}{\partial d}$ is the change in electrostatic force due to the moving finger displacement, and is therefore proportional to V^2. $\frac{\partial F_M}{\partial F_E}$ is the amount which a structure moves due to a change in applied force, and is inversely proportional to the stiffness of the structural material. Therefore, the lumped-model self-consistent scheme converges if either the tether is stiff enough or the applied voltage

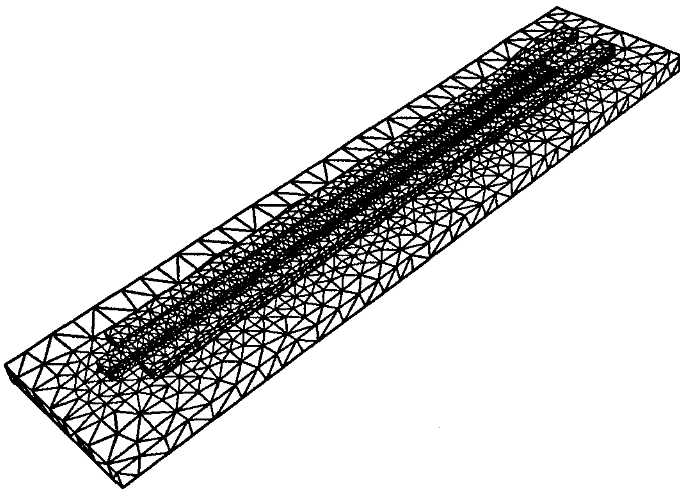

Figure 6: 3-D FastCap mesh of a unit cell.

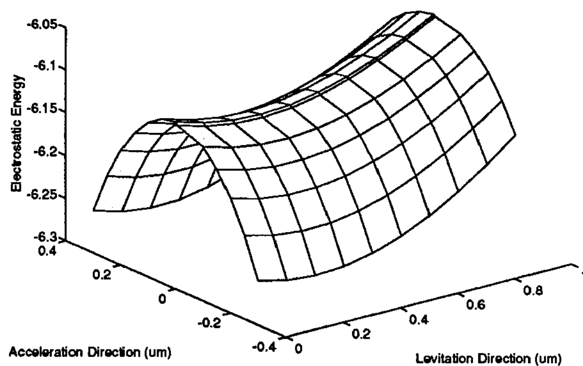

Figure 7: Electrostatic energy distribution.

is small enough. In other words, the lumped-model self-consistent analysis scheme converges for a stable structure. Fortunately, for the surface micro-machined accelerometer, the tether structure is designed to be stiff enough in comparison to the applied voltage (< 5v) to assure stability. However, for an unstable structure, there is no stable balance state (aside from contact between the fixed and moving fingers) and the lumped-model self-consistent analysis scheme diverges. Fig. 8 demonstrates that making the structure more stiff by increasing the residual tensile stress of the ADXL50 structure's tether leads to faster convergence.

4 Resonant Frequency Measurement and Analysis

One of the most useful parameters for an accelerometer is its fundamental resonant frequency. It gives a practical upper bound on the system bandwidth and in the case of surface micromachined structures is indicative of the mechanical compliance and thus the accelerometer's sensitivity. However, because the applied bias voltages create electrostatic forces which act in opposition to the spring forces and thus "soften" the mechanical compliance, the actual resonant frequency is lower than the pure mechanical resonant frequency. Knowledge of the difference between the electromechanical and pure mechanical resonant frequencies is of great significance in the design process.

The resonant frequency of several open-loop ADXL50 accelerometers were measured as a function of the applied DC bias voltages on the structure. In order to make the most accurate measurement of the electromechanical resonant frequency, we used a special open-loop version of the ADXL50 accelerometer. In essence, this device only contains the mechanical structures and an output buffer amplifier. The signals applied to the fixed fingers and moving mass were applied via external sources and were equivalent to the normal operating voltages described earlier, except for the follow differences. First, the DC bias voltages are not fixed, but rather are the varied parameters in the measurement. Second, in order to measure the resonant frequency, a small (100mV peak) AC sinusoidal signal is superimposed on the DC bias of the moving mass to excite a sinusoidal motion. This AC signal is swept through the frequency range of interest by a Hewlett-Packard Model 3589A Spectrum Analyzer. Using the output signal, the analyzer plots the frequency response of the system. The peak frequency is then chosen as the resonant frequency for the given set of DC bias voltages. Because the applied AC sweep signal causes electrostatic forces which could effect the resonant frequency, a second measurement method was used to confirm the initial measurements. In this method, the accelerometer was evacuated and the random Brownian noise spectrum was observed. The peak of this spectrum is the resonant frequency. Both methods yielded essentially identical resonant frequency values.

Figure 9 shows the resonant frequency data versus the DC bias voltage difference on the fixed fingers. The DC bias voltage on the horizontal axis of Fig. 9 was applied to the right-hand fixed finger of each finger cell (see Fig. 1). The left-hand fixed finger was grounded. The DC potential of the moving mass and its fingers (as well as the ground-plane under the structure) was centered between these values (ie, one-half the horizontal-axis potential). The change in resonant frequency with applied DC bias voltage in Fig. 9 is caused by the reduction in the effective spring constant due to the electrostatic forces.

Considering the actual fabricated structure, including over-etching, warpage, and the residual stress in the tethers, the electromechanical resonant frequency was calculated for the ADXL50 structure (Fig. 3) using the lumped-model self-consistent analysis algorithm. In this calculation, the thickness of the structural poly-silicon is 2 μm, the Young's Modulus is 1.61×10^{11} Pa, the Poisson ratio is 0.226, the material density is 2.3×10^3 Kg/m^3 yielding a total moving mass of 1.65×10^{-10} Kg, the average over-etching is 0.15 μm, and the average residual stress in the tethers is 54 MPa. The warpage was modeled as previously described. Fig. 9 shows good agree-

ment between the simulated resonant frequency versus DC bias and the measured values described above. Note that the value used for the tether average residual stress, 54 MPa, was essentially used as a fitting parameter. However, the average residual stress for dozens of wafer lots was measured (by a wafer curvature measurement) to be 58 MPa with a standard deviation of 4 MPa. Considering that we have used average values for the Young's Modulus and the over-etching, as opposed to actual values, this level of variation can be considered small.

Conclusions

Using a simple analysis technique, the stability and the effects of structure misalignment on a surface-micromachined accelerometer were predicted, saving considerable time and expense for prototype fabrication. The lumped-model self-consistent analysis method allowed quick and computationally practical simulations of complex surface-micromachined structures with typical fabrication non-idealities, such as structure warpage. The method was demonstrated here by the accurate prediction of a surface micromachined accelerometer's resonant frequency, which is a critical parameter for the system design.

Acknowledgments

The authors would like to thank the members of the MIT MEMCAD group for many valuable discussions. In addition, we thank Kevin Chau, Steve Lewis, Jack Memishian and Yang Zhao, all of Analog Devices, for help with the resonant frequency measurement techniques and circuitry. Thanks also go to Terry Core of Analog Devices for providing the residual stress data. This work was supported by the Defense Advanced Research Projects Agency contracts J-FBI-92-196 and DABT63-93-C-0065, the National Science Foundation contract MIP-8858764 A02, the SRC contract 92-SP-309, grants from I.B.M. and Digital Equipment Corporation, and Analog Devices, Inc.

References

[1] F. Goodenough, "Combining Micromachining with Analog IC Technology", Electronic Design, August 8, 1991.

[2] S. Sherman, W. Tsang, T. Core, R. Payne, D. Quinn, K. Chau, J. Farash, S. Baum, "A Low Cost Monolithic Accelerometer; Product/Technology Update", *Proc. IEEE 1992 Int. Elec. Dev. meeting,* San Francisco, CA, Dec. 13-16, 1992, pp. 19.1.1–19.1.4.

[3] X. Cai, P. Osterberg, H. Yie, J. Gilbert, S. Senturia and J. White, "Self-Consistent Electromechanical Analysis of Complex 3-D Microelectromechanical Structures Using a Relaxation/Multipole-Accelerated Method," Invited paper to appear in the Journal of Microelectromechanical Systems.

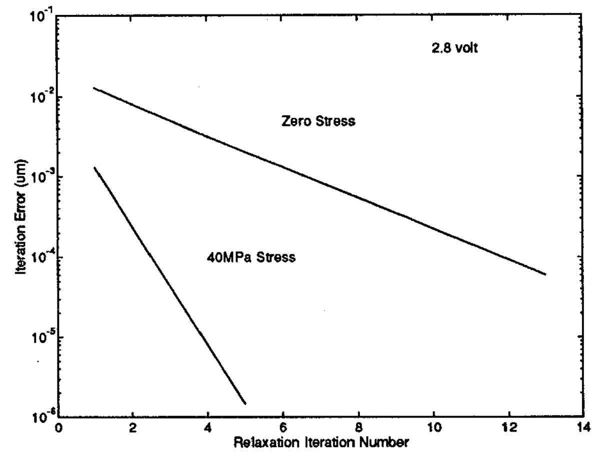

Figure 8: Lumped-model convergence for different tether tensile stresses.

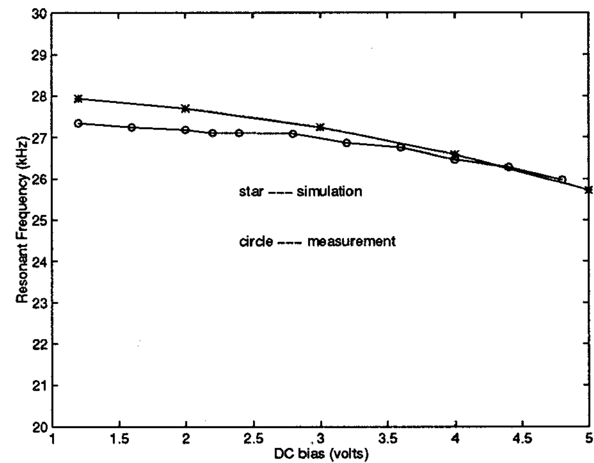

Figure 9: Resonant frequency versus DC bias.

[4] Hibbit, Karlsson, and Sorensen, Inc., Providence, R.I.

[5] K. Nabors and J. White, "FastCap: A multipole-accelerated 3-D capacitance extraction program," *IEEE Transactions on Computer-Aided Design*, vol. 10, Nov. 1991, p1447-1459.

[6] J.M.Ortega and W.C.Rheinboldt, *Iterative Solution of Nonlinear Equations in Several Variables.* Academic Press, Inc., 1970, San Diego, CA.